

The potential of using Landsat 7 data for the classification of sea ice surface conditions during summer

Thorsten Markus

Mail Code 971

NASA Goddard Space Flight Center - Univ. Maryland, Baltimore County

Joint Center for Earth Systems Technology

Greenbelt, MD 20771

Tel.: +1-301-614-5882

Fax: +1-301-614-5644

email: Thorsten.Markus.1@gsfc.nasa.gov

Donald J. Cavalieri

Laboratory for Hydrospheric Processes/Code 971

NASA Goddard Space Flight Center

Greenbelt, MD 20771

Alvaro Ivanoff

Raytheon ITSS Corporation

4400 Forbes Blvd.

Lanham, MD 20706

Submitted to the *Annals of Glaciology*

Significance

The significance of this paper is that the potential for mapping melt ponds over Arctic sea ice using Landsat 7 ETM+ imagery has been demonstrated for the first time. This result will greatly enhance the utility of this sensor for EOS Aqua AMSR-E sea ice validation studies. The analysis shows that different surface conditions, such as wet snow and melt-ponded areas, have different signatures in the individual ETM+ bands. Consistent with in-situ albedo measurements, melt ponds, show up as bluish, whereas dry and wet ice have a white to gray appearance in the ETM+ true-color images. These spectral differences demonstrate the potential of using ETM+ imager for mapping the distribution of melt ponds and other surface conditions during Arctic summer. For the image analyzed in this paper, the melt pond fraction was calculated to be 37%. This work supports NASA's EOS algorithm development and validation activities.

The potential of using Landsat 7 data for the classification of sea ice surface conditions during summer

Thorsten Markus

Mail Code 971

NASA Goddard Space Flight Center - Univ. Maryland, Baltimore County

Joint Center for Earth Systems Technology

Greenbelt, MD 20771

Tel.: +1-301-614-5882

Fax: +1-301-614-5644

email: Thorsten.Markus.1@gsfc.nasa.gov

Donald J. Cavalieri

Laboratory for Hydrospheric Processes/Code 971

NASA Goddard Space Flight Center

Greenbelt, MD 20771

Alvaro Ivanoff

Raytheon ITSS Corporation

4400 Forbes Blvd.

Lanham, MD 20706

Submitted to the *Annals of Glaciology*

Popular Summary

During spring and summer, the surface of the Arctic sea ice cover undergoes rapid changes that greatly affect the surface albedo and significantly impact the further decay of the sea ice. These are primarily the development of a wet snow cover and the development of melt ponds. As the melt pond diameter generally does not exceed a couple of meters, the spatial resolutions of sensors like NOAA AVHRR and EOS Terra MODIS are too coarse for their identification. Landsat 7 ETM+, on the other hand, has a spatial resolution of 30 m (15 m for the panchromatic band). The different wavelengths (bands) from blue to near-infrared offer the potential of distinguishing among different surface conditions. Landsat 7 ETM+ images obtained during June 2000 for the Baffin Bay region have been analyzed. The analysis shows that different surface conditions, such as wet snow and melt-ponded areas, have different signatures in the individual ETM+ bands. Consistent with in-situ albedo measurements, meltponds, show up as bluish, whereas dry and wet ice have a white to gray appearance in the Landsat true-color images. These spectral differences demonstrate the potential of using ETM+ imager for mapping the distribution of melt ponds and other surface conditions during Arctic summer. For the image analyzed in this paper, the melt pond fraction was calculated to be 37%.

The potential of using Landsat 7 ETM+ for the classification of sea ice surface conditions during summer

Thorsten Markus

Mail Code 971

NASA Goddard Space Flight Center - Univ. Maryland, Baltimore County

Joint Center for Earth Systems Technology

Greenbelt, MD 20771

Tel.: +1-301-614-5882

Fax: +1-301-614-5644

email: Thorsten.Markus.1@gsfc.nasa.gov

Donald J. Cavalieri

Laboratory for Hydrospheric Processes/Code 971

NASA Goddard Space Flight Center

Greenbelt, MD 20771

Alvaro Ivanoff

SSAI/NASA Goddard Space Flight Center/Code 971

Greenbelt, MD 20771

Abstract

During spring and summer, the surface of the Arctic sea ice cover undergoes rapid changes that greatly affect the surface albedo and significantly impact the further decay of the sea ice. These changes are primarily the development of a wet snow cover and the development of melt ponds. As melt pond diameters generally do not exceed a couple of meters, the spatial resolutions of sensors like AVHRR and MODIS are too coarse for their identification. Landsat 7, on the other hand, has a spatial resolution of 30 m (15 m for the pan-chromatic band). The different wavelengths (bands) from blue to near-infrared offer the potential to distinguish among different surface conditions. Landsat 7 data for the Baffin Bay region for June 2000 have been analyzed. The analysis shows that different surface conditions, such as wet snow and meltponded areas, have different signatures in the individual Landsat bands. Consistent with in-situ albedo measurements, melt ponds show up as blueish whereas dry and wet ice have a white to gray appearance in the Landsat true-color image. These spectral differences enable the distinction of melt ponds. The melt pond fraction for the scene studied in this paper was 37%.

Introduction

Melt ponds and wet snow cover a significant area of the summer Arctic sea ice. Melt features on sea ice can cover more than 50% of the sea ice area [*Derksen et al.*, 1997; *Fetterer and Untersteiner*, 1998]. As the albedo of wet snow and melt ponds is considerably lower than the albedo of dry ice (down to 0.2 for 30 cm deep ponds [*Grenfell and Maykut*, 1977]), accurate classification of those is essential for estimates of the polar summer time energy balance.

Perovich et al. [1986] measured the spectral albedos of dry snow, wet snow, and melt ponds at several depths. Whereas wet snow reduces the spectral albedo, compared to dry snow, by about the same value over the whole visible range, melt ponds have a greater reduction at longer wavelengths and therefore appear blueish. The spectral albedo of melt ponds for wavelengths greater than 800 nm is about 0.05 independent of melt pond depth whereas at 500 nm, the albedo decreases from 0.6 for an early season 0.1 m deep melt pond to 0.25 for a 0.3 m deep old melt pond. These relative higher blue albedos have also been observed by *Barber and Yackel* [1999] and *Morassutti and LeDrew* [1996]. *Tschudi et al.* [1997] made use of this spectral difference to identify melt ponds using video data.

For larger spatial areas, the Landsat7 Enhanced Thematic Mapper (ETM+) is an excellent sensor with which to study the surface properties of sea ice during summer. In addition to the different spectral bands, covering the range from 450 nm (blue) to near-infrared and also thermal infrared, the data have a spatial resolution of 30 m (15 m for the pan-chromatic band) (Table 1). This high spatial resolution is necessary to enable the identification of melt ponds as melt ponds commonly have diameters of a couple of meters. although melt ponds as large as 400 m across have been measured [*Fetterer and Untersteiner*, 1998].

As part of the pre-launch summer Arctic Aqua AMSR-E validation aircraft campaign Meltpond2000 in June/July 2000 [*Cavalieri*, 2000], four cloud-free Landsat7

scenes over Baffin Bay were acquired (Figure 1). Here, we look in detail at one scene (Scene 2 in Figure 1) that consists of large number of different surface types. Baffin Bay is a good area for this initial investigation as it does not contain any multiyear ice so that we only have one primary ice type and the observed different signatures result from variations in the surface properties only.

Analysis

Figure 2 shows a true-color Landsat scene of Baffin Bay where bands 3,2,1 are red, green, and blue, respectively. Additionally, clouds as detected using band 7 are indicated in red. The two boxes indicate areas studied in more detail.

Spectral analysis of melt features

Figure 3 shows a full resolution subset as indicated by the red box in Figure 1. One can clearly distinguish between open water and individual ice floes. Whereas open water has a very distinct signature, the summertime brightness of sea ice varies significantly. Dry ice is seen as white, but with the onset of melt and the consequent wetting of the snow/ice cover, the signatures vary considerably. As mentioned above, melt ponds (at least shallow melt ponds) appear as light blue in the true color images (point A). Additionally, one can identify different shades of blue (points B–D) that are clearly separate from different shades of gray (points E–H). This is even more distinct in the contour scatterplots of band 1 vs band 3 and band 1 vs band 4 (Figure 4). The general ice-water line ranges from point E (white ice) to point H (open water). The points F and G, which also lie on this line, represent wet snow or remains of decaying sea ice. The heavy population of pixels with values of 255 in band 1 results from saturation in the high-gain Landsat data. According to *Perovich et al.* [1986], a wet snow cover shifts the albedo by about the same value for the whole visible range. When melt ponds develop, on the other hand, shorter wavelengths remain relatively higher compared to the longer

wavelength. Thus, pixels will deviate from the dry ice-open water line towards higher band 1 (blue) values, and presumably move from point A to point D as the melt pond depth increases.

When plotting brightness (or rather DN value) versus wavelength (Figure 5), one notices that, in agreement with the measurements from *Perovich et al.* [1986], melt pond pixels (A–D: solid lines) have a greater gradient than points E–H (dotted lines). Also in agreement with their measurements, at wavelengths longer than 800 nm melt pond pixels (except for point A) have about the same brightness. Furthermore, the gradient between bands 2 and 3 is clearly negative for melt ponds, whereas the gradient for white and wet ice is very close to zero. This spectral dependence makes sea ice surface classification possible. Figure 6 shows a classified image where open water is black, dry and wet ice are white, and melt ponds are gray. For melt pond areas the gradient between band 2 and band 3 is greater than 10. The melt pond fraction for this particular subscene is 37%. It seems that estimates of melt pond depth are possible but further investigations, for example the comparison of Landsat signatures with in-situ measurements of melt ponds at different stages, are needed.

Melt features in the pan-chromatic channel

Although different surface types can have similar gray values when using single-channel instruments [*Derkson et al.*, 1997] (making the distinction between melt ponds and wet surfaces difficult), the use of the very high resolution (15 m) pan-chromatic channel (band 8) may be desirable particularly for ice concentration estimates [see *Cavalieri et al.*, this issue]. In Figure 3, the “darkest” sea ice areas are represented by points D and G, and yet their spectral signatures are different, indicating different surface types (deep melt ponds versus very wet snow or remains of decaying sea ice; see discussion above). Despite these spectral differences, both surface types have similar DN values of around 60 in the pan-chromatic band. Thus, neglecting pixels consisting

of mixtures of open water and dry ice, a value of 60 seems to be a valid lower threshold of sea ice during summer.

Clouds and cloud shadows

At least for summer conditions, bands 5 and 7 can be used for cloud detection as the cloud top temperature is colder than the surface temperature. Figure 6a shows a subset of Figure 2 as indicated by the black box. The clouds in band 7 appear bright (Figure 6b). Comparison of the true-color image with the band 7 subset reveals that the cloud band itself do not affect the albedos directly. No variation in brightness can be detected for the pixels where band 7 detects clouds. It is the shadow of the clouds that causes a darkening in the visible bands (above the cloud band in Figure 6a). All bands show a reduction in brightness for the cloud shadow region. The difference between band 2 and 3 is greater compared to the cloud-free area. Scatterplots indicate that cloud shadow pixels and melt pond pixels have similar spectral signatures. Thus, these shadows would be misclassified as melt ponded. As we do not have a satisfying procedure to identify cloud shadows yet, careful visual inspection is necessary before applying any algorithm.

Conclusions

This study has demonstrated the great potential inherent in Landsat7 ETM+ data for the classification of summertime sea ice surface conditions. Melt ponds can easily be distinguished from dry and wet ice by their blueish appearance and by their greater negative spectral gradients between bands 2 and 3. Estimates of melt pond depths are likely possible but further investigations are needed to develop a broader range of case studies and to acquire coincident in-situ measurements for enabling a detailed analysis of melt pond signatures in the ETM+ data. Whereas clouds can be detected using bands 5 or 7, cloud shadows have spectral signatures similar to melt ponds and therefore have to be detected visually before large-scale operational analyses can be carried out.

References

- Barber, D.G., and J. Yackel, The physical, radiative, and microwave scattering characteristics of melt ponds on Arctic land fast ice, *Int. J. Remote Sensing*, **20**, 2069-2090, 1999.
- Cavalieri, D.J., EOS Aqua AMSR-E Sea Ice Validation Program: Meltpond2000 Flight Report, *NASA/TM-2000-209972*, 31pp., 2000.
- Cavalieri, D.J., T. Markus, and A. Ivanoff, Comparisons of DMSP SSM/I and Landsat7 ETM+ sea ice concentrations during summer melt, *this issue*, 2001.
- Derksen, C, J. Piwowar, and E. LeDrew, Sea-ice melt-pond fraction as determined from low level aerial photographs, *Arctic and Alpine Research*, **29**, 345-351, 1997.
- Grenfell, T.C., and G.A. Maykut, The optical properties of ice and snow in the Arctic Basin, *J. Glaciol*, **18**, 445-463, 1977.
- Fetterer, F., and N. Untersteiner, Observations of melt ponds on Arctic sea ice, *J. Geophys. Res.*, **103**, 24,821-24,835, 1998.
- Morassutti, M.P., and E.F. LeDrew, Albedo and depth of melt ponds on sea ice, *Int. J. Clim.*, **16**, 817-838, 1996.
- Perovich, D.K., G.A. Maykut, and T.C. Grenfell, Optical properties of ice and snow in the polar oceans. I: observations, *SPIE, Vol.637 Ocean Optics VIII*, 232-241, 1986.
- Tschudi, M.A., J.A. Curry, and J.A. Maslanik, Determination of areal surface-feature coverage in the Beaufort Sea using aircraft video data, *Ann. Glaciol.*, **25**, 434-438, 1997.

Table 1. Landsat characteristics.

Band no.	bandwidth [nm]	FOV [m]	Sample distance [m]
1	450–515	30	30
2	525–605	30	30
3	630–690	30	30
4	750–900	30	30
5	1550–1750	30	30
6	10400–12500	30	60
7	2090–2350	30	30
8	520–900	13×15	15

Figure 1. Overview of the Landsat scenes acquired for June 26/27, 2000.

Figure 2. Landsat true color image of Baffin Bay for June 26, 2000. (Bands 3,2,1 for red,green,and blue, respectively.) Clouds, as detected by band 7, are shaded in red. The red and black boxes indicate areas studied in detail.

Figure 3. Full resolution subscene of Figure 2 (red box). The dimensions are 1000 × 1000 30-m pixels. The labels A-D indicate typical different shades of blue; the labels E-H indicate different gray levels.

Figure 4. Distribution of Landsat pixels; band 3 vs band 1 (a) and band 4 vs band 1 (b). The labels correspond to the labels in Figure 3.

Figure 5. Landsat brightness (DN) values versus wavelength. The solid lines are for points A-D in decreasing brightness; the dotted lines are for points E-H in decreasing brightness.

Figure 6. Automatically classified image of the Landast scene in Figure 3. Open water is black, dry and wet ice is white, and melt ponds are gray.

Figure 7. True-color subscene of Figure 2 (black box) (a), and band 7 image for the same area (b).

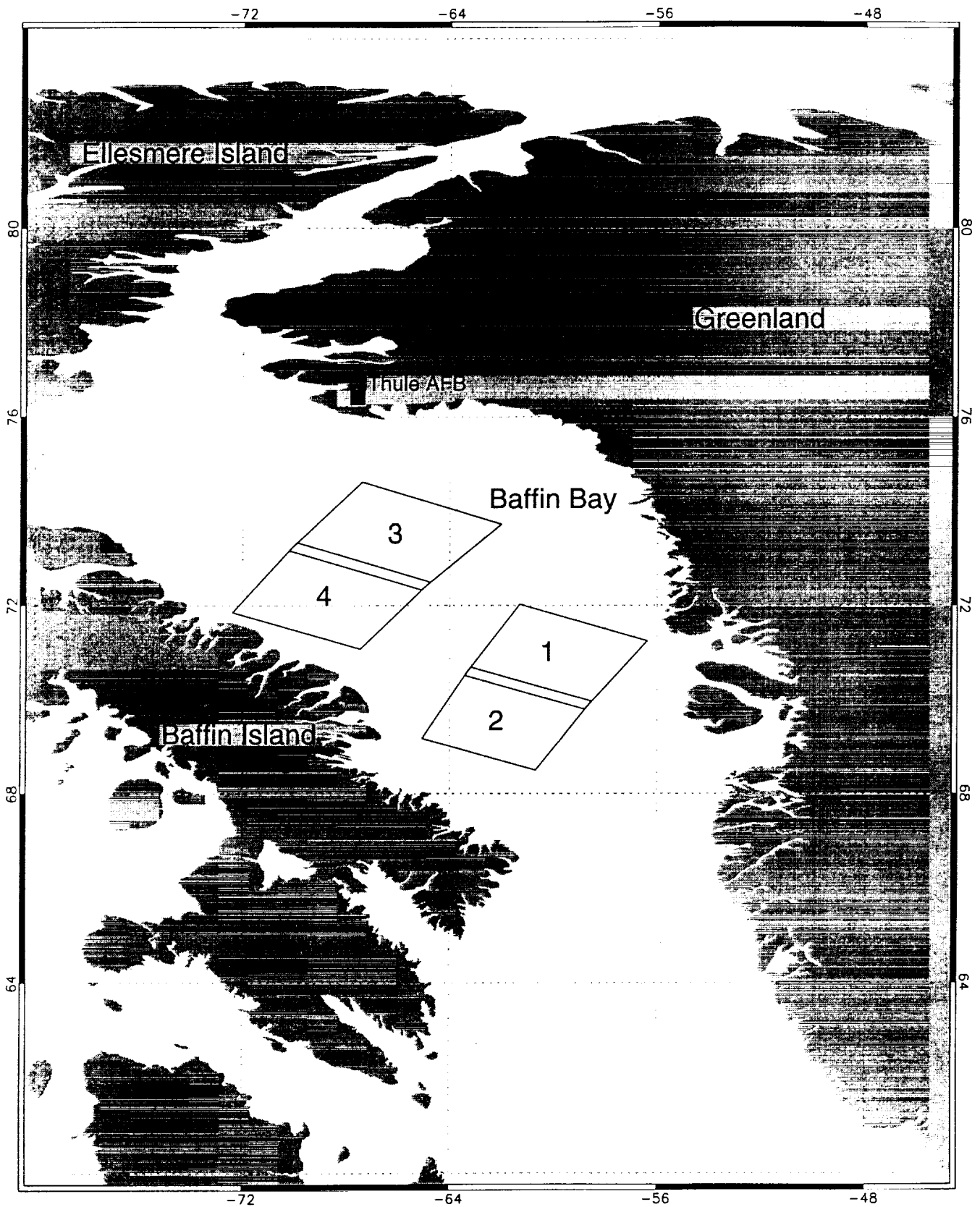


Fig. 1

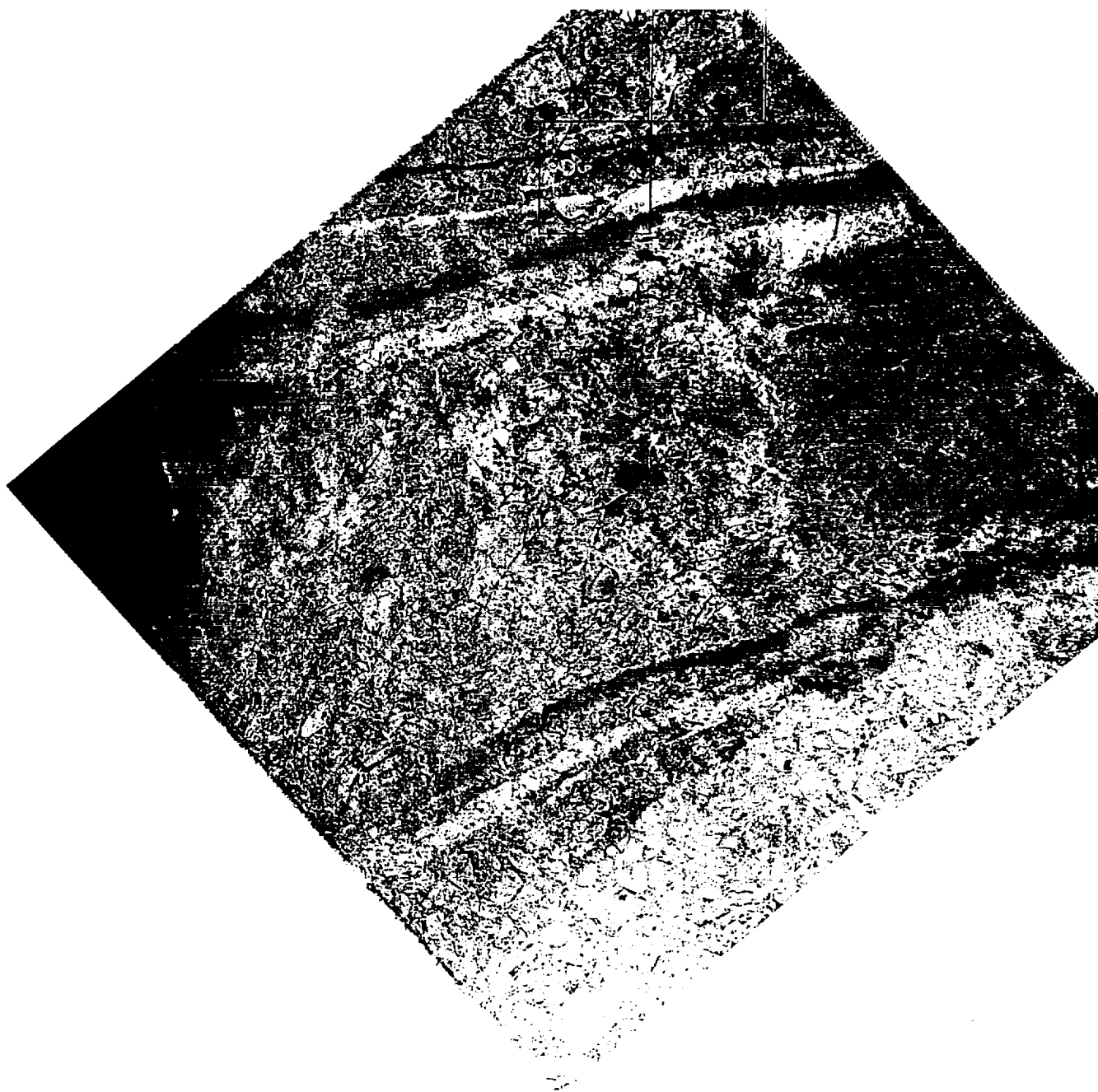


Fig. 2

491

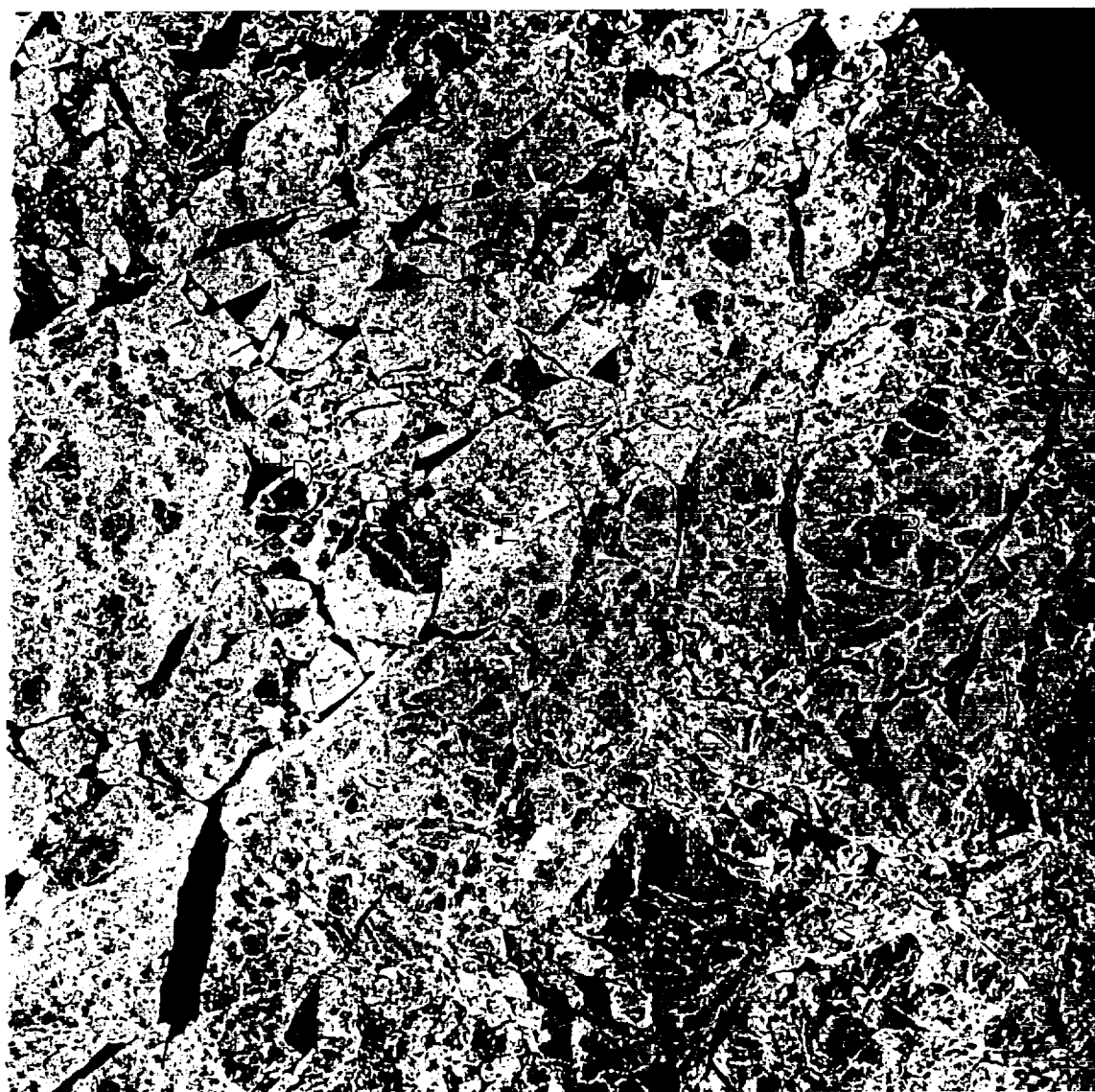


Fig. 3

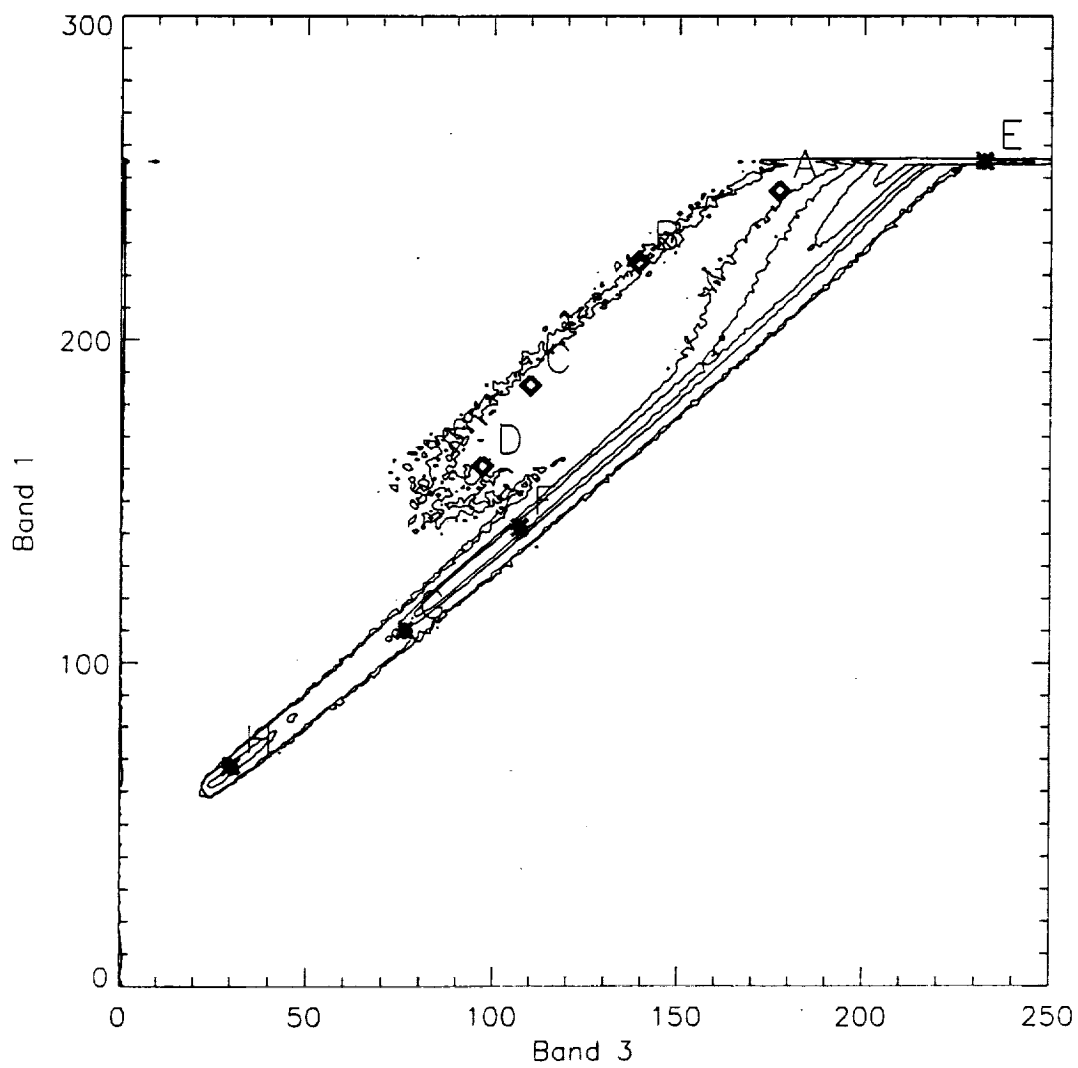


Fig. 4a

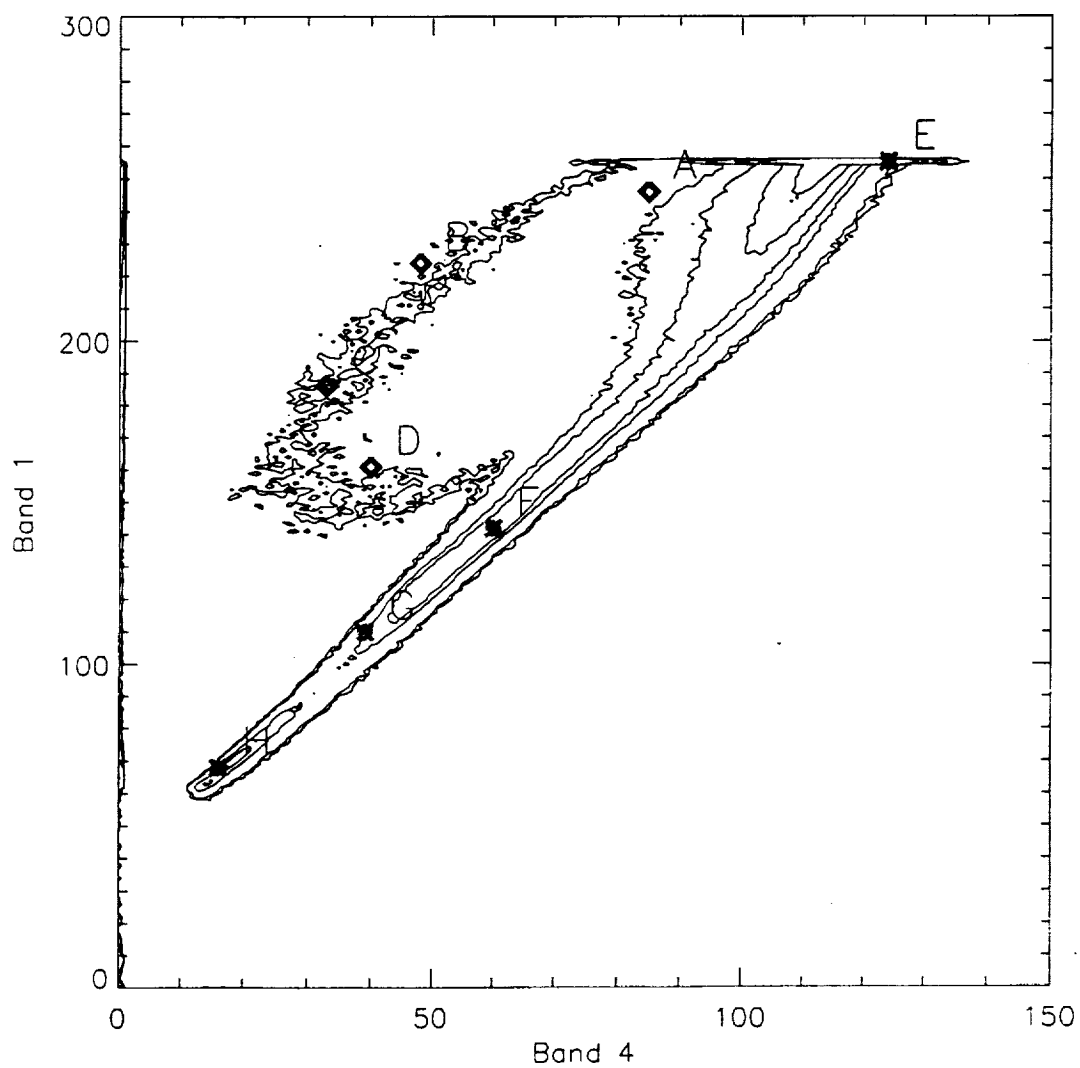


Fig. 46

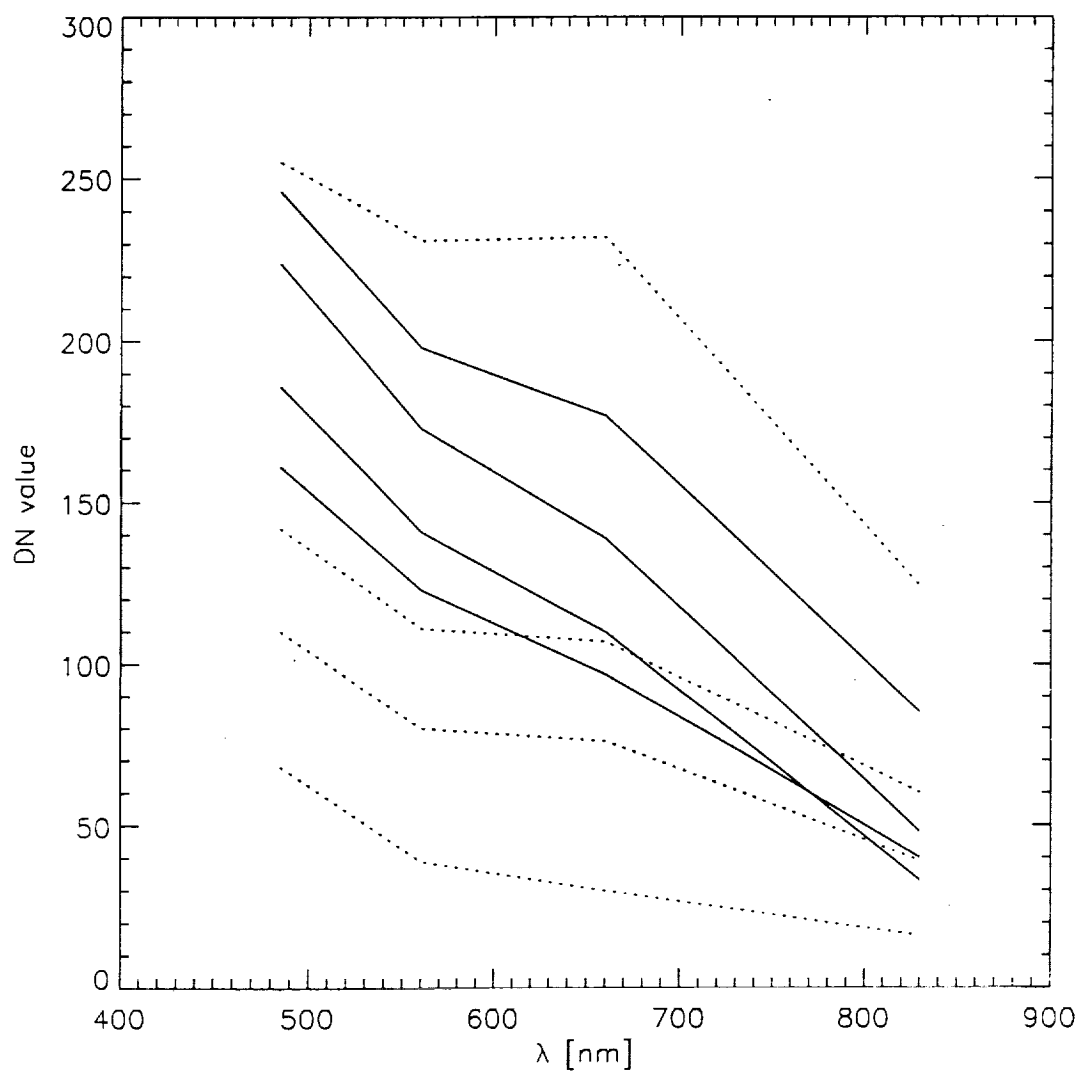


Fig. 5

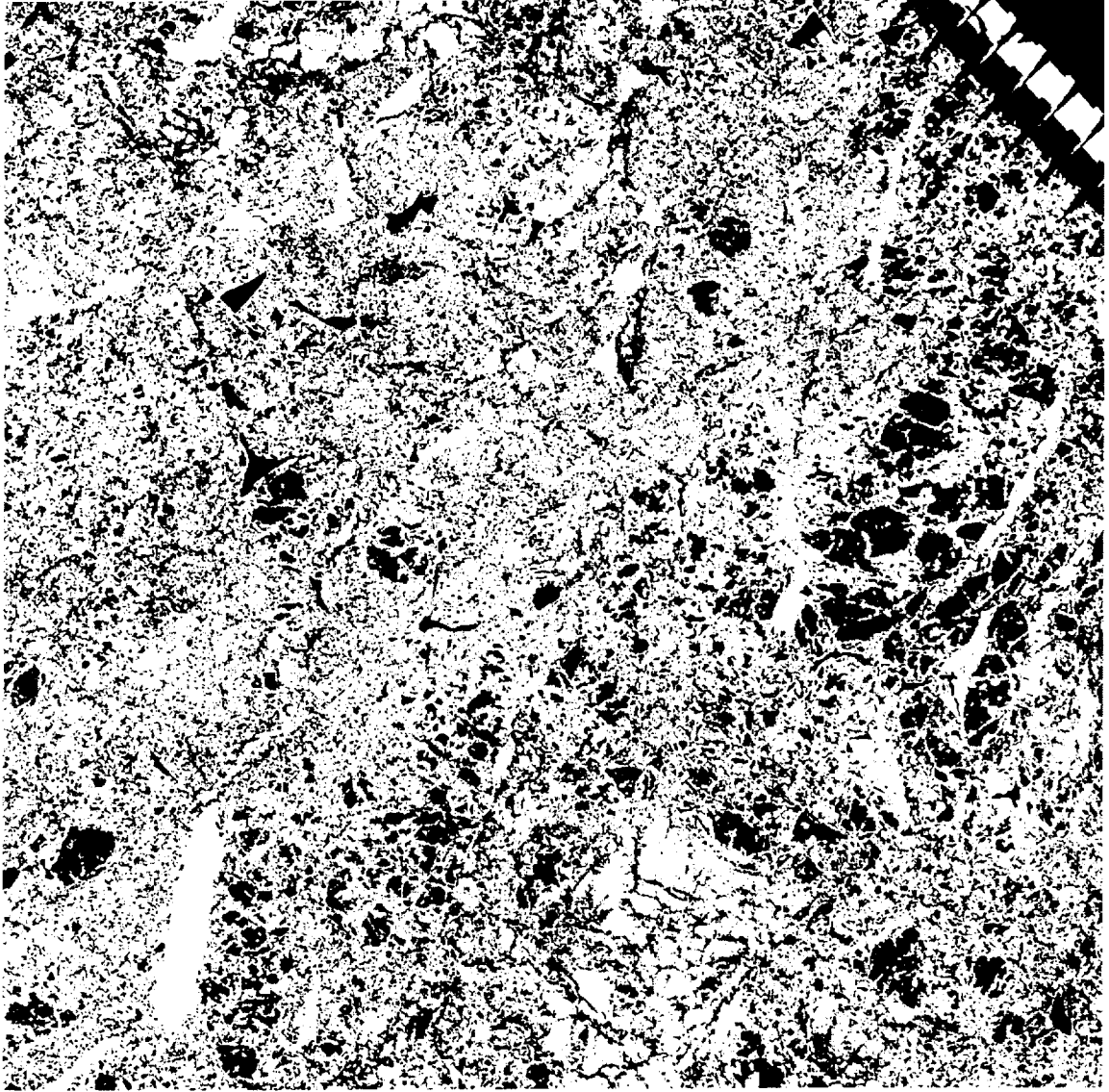
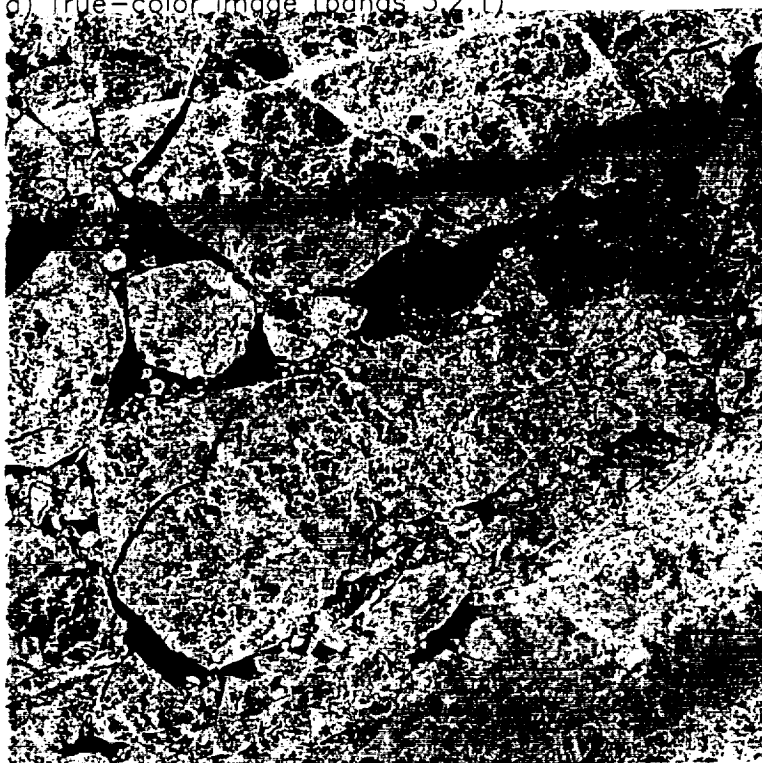


Fig. 6

a) True-color image (bands 3,2,1)



b) Band 7 image

